

Discovery of VU6005649, a CNS Penetrant mGlu7/8 Receptor PAM Derived from a Series of Pyrazolo[1,5-a]pyrimidines

Masahito Abe, Mabel Seto, Rocco G Gogliotti, Matthew T. Loch, Katrina A Bollinger, Sichen Chang, Eileen M Engelberg, Vincent B Luscombe, Joel Harp, Michael Bubser, Darren W. Engers, Carrie K. Jones, Alice L Rodriguez, Anna L. Blobaum, Jeff Conn, Colleen M Niswender, and Craig W Lindsley

ACS Med. Chem. Lett., **Just Accepted Manuscript** • DOI: 10.1021/acsmedchemlett.7b00317 • Publication Date (Web): 01 Sep 2017

Downloaded from <http://pubs.acs.org> on September 4, 2017

Just Accepted

"Just Accepted" manuscripts have been peer-reviewed and accepted for publication. They are posted online prior to technical editing, formatting for publication and author proofing. The American Chemical Society provides "Just Accepted" as a free service to the research community to expedite the dissemination of scientific material as soon as possible after acceptance. "Just Accepted" manuscripts appear in full in PDF format accompanied by an HTML abstract. "Just Accepted" manuscripts have been fully peer reviewed, but should not be considered the official version of record. They are accessible to all readers and citable by the Digital Object Identifier (DOI®). "Just Accepted" is an optional service offered to authors. Therefore, the "Just Accepted" Web site may not include all articles that will be published in the journal. After a manuscript is technically edited and formatted, it will be removed from the "Just Accepted" Web site and published as an ASAP article. Note that technical editing may introduce minor changes to the manuscript text and/or graphics which could affect content, and all legal disclaimers and ethical guidelines that apply to the journal pertain. ACS cannot be held responsible for errors or consequences arising from the use of information contained in these "Just Accepted" manuscripts.



Discovery of VU6005649, a CNS Penetrant mGlu_{7/8} Receptor PAM Derived from a Series of Pyrazolo[1,5-*a*]pyrimidines

Masahito Abe,^{†,‡,§} Mabel Seto,^{†,‡,§} Rocco G. Gogliotti,^{†,‡,§} Matthew T. Loch,^{†,‡} Katrina A. Bollinger,[‡] Sichen Chang,[‡] Eileen M. Engelberg,^{†,‡} Vincent B. Luscombe,^{†,‡} Joel M. Harp,[§] Michael Bubser,^{†,‡} Darren W. Engers,^{†,‡} Carrie K. Jones,^{†,‡,‡} Alice L. Rodriguez,^{†,‡} Anna L. Blobaum,^{†,‡} P. Jeffrey Conn,^{†,‡,‡} Colleen M. Niswender,^{†,‡,‡*} and Craig W. Lindsley^{†,‡,‡*}

[†]Department of Pharmacology, Vanderbilt University School of Medicine, Nashville, TN 37232, United States

[‡]Vanderbilt Center for Neuroscience Drug Discovery, Vanderbilt University School of Medicine, Nashville, TN 37232, United States

[§]Department of Biochemistry, Vanderbilt University School of Medicine, Nashville, TN 37232, USA

[‡]Vanderbilt Kennedy Center, Vanderbilt University Medical Center, Nashville, TN 37232, USA

[§]These three authors contributed equally; *Co-corresponding authors

KEYWORDS: Positive allosteric modulator (PAM), metabotropic glutamate receptor 7 (mGlu₇), cognition, VU6005649, Rett syndrome

ABSTRACT: Herein, we report the structure-activity relationships within a series of mGlu₇ PAMs based on a pyrazolo[1,5-*a*]pyrimidine core with excellent CNS penetration ($K_{p,s} > 1$ and $K_{p,u,s} > 1$). Analogs in this series proved to display a range of Group III mGlu receptor selectivity, but VU6005649 emerged as the first dual mGlu_{7/8} PAM, filling a void in the Group III mGlu receptor PAM toolbox, and demonstrating *in vivo* efficacy in a mouse contextual fear conditioning model.

Of the eight metabotropic glutamate receptors (mGlu_s) and their associated three groups (Group I: mGlu_{1,5}, Group II: mGlu_{2,3}, Group III: mGlu_{4,6,7,8}), mGlu₇ and mGlu₈ remain the least explored due to a lack of selective small molecule tools.^{1,2} Of these, mGlu₇ has emerged as an attractive therapeutic target for anxiety, depression, epilepsy and schizophrenia based on data from mGlu₇ knock-out (KO) mice.³⁻¹¹ Human genetics has further strengthened these associations, with *GRM7* polymorphisms linked to schizophrenia, depression, ADHD, and autism.¹²⁻²³ Additionally, whole exome sequencing approaches have recently identified mutations in the *GMR7* gene in patients with previously diagnosed neurodevelopmental disorders.^{8,23-25} Finally, we have recently described dramatic reductions in mGlu₇ protein expression in the brains of patients diagnosed with Rett syndrome (RTT),²⁶ as well as mice modeling the disorder, and that nonselective positive allosteric modulators (PAMs) with mGlu₇ activity can correct apneas as well as numerous impaired cognitive and social domains in mice modeling RTT.²⁶

mGlu₇ is broadly expressed in the CNS where it critically modulates synaptic transmission and neuronal function.¹

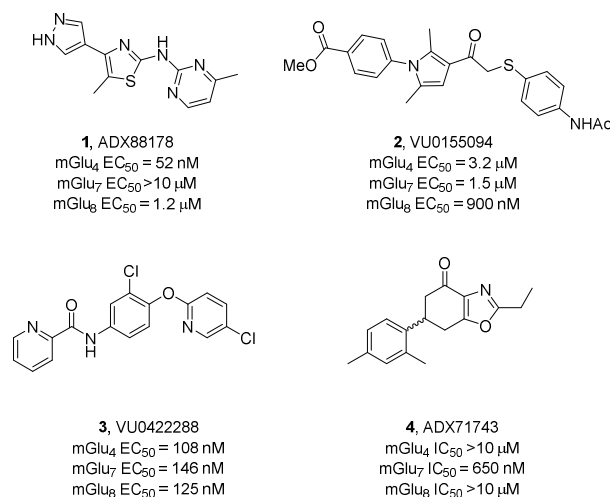


Figure 1. Structures of reported Group III mGlu receptor allosteric ligands. ADX88178 (1) is an mGlu_{4/8} PAM, VU0155094 (2) is a *pan*-Group III (mGlu_{4/7/8}) PAM, VU0422288 (3) is a potent *pan*-Group III (mGlu_{4/7/8}) PAM, and ADX71743 (4) is a selective mGlu₇ NAM. No mGlu₇ selective or preferring PAMs have been disclosed to date. Potencies were determined in-house.

Due to a lack of mGlu₇-selective small molecule tools, recent efforts, including our own, have employed non-selective, *pan*-Group III mGlu receptor (PAMs) in combination with synaptic

localization studies, mGlu₇ negative allosteric modulators (NAM), and/or *Grm7*^{-/-} mice to ‘isolate’ selective mGlu₇ activation.^{23,27} As shown in Figure 1, all PAM ligands reported to date are not selective for mGlu₇ (e.g., **1** is an mGlu_{4/8} PAM and both **2** and **3** are *pan*-mGlu_{4/7/8} PAMs), while **4** is a selective mGlu₇ NAM.^{1,2,26,27,28, 29 and in house data} Thus, our lab initiated a campaign to discover and optimize selective and CNS penetrant mGlu₇ PAMs for target validation studies. Here, we detail a new high-throughput screening (HTS) campaign that identified a novel series of pyrazolo[1,5-*a*]pyrimidines as mGlu₇-preferring and dual mGlu_{7/8} PAMs with excellent CNS penetration and *in vivo* efficacy in a mouse contextual fear conditioning model.

We performed an HTS campaign on a collection of 63,000 small molecules and identified 438 hits as mGlu₇ PAMs in a single point screen.² After single-point hit confirmation, counter-screening against untransfected HEK cells and full concentration-response curve confirmation, 98 compounds were confirmed as mGlu₇ PAMs. Hits with attractive chemotypes were then evaluated against mGlu₄ and mGlu₈; HTS hit **5** (Figure 2), based on a pyrazolo[1,5-*a*]pyrimidine core, proved worthy of further attention. Hit **5** was selective for mGlu₇ (mGlu₇ EC₅₀ = 3.3 μM, pEC₅₀ = 5.48±0.14, 104±5 Glu Max, mGlu₄ EC₅₀ >10 μM, mGlu₈ EC₅₀ >10 μM) and displayed exceptional CNS penetration (rat plasma:brain K_p = 1.4, K_{p,uu} = 1.1). From an optimization standpoint, **5** was also attractive in that multiple domains could be surveyed in parallel.

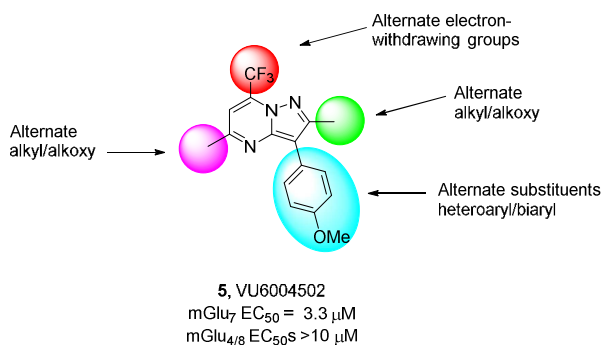
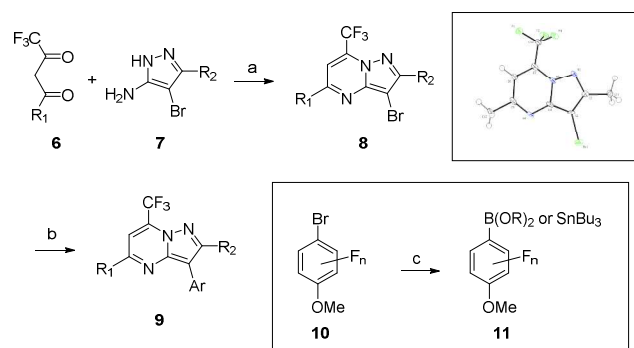


Figure 2. Structure of HTS hit **5** (VU6004502), and the four domains to be investigated in the course of the lead optimization campaign.

The synthesis of **5** and related analogs **9** was straightforward (retaining the CF₃ moiety) and required only two steps from known materials (Scheme 1) when the requisite boronic acid was commercial.³⁰ In other cases, the desired coupling partner (either aryl boronic acid or aryl stannane **11**) was prepared from the corresponding commercial aryl bromides **10**. However, this streamlined strategy hinged on a successful condensation of **6** and **7** to form **8** as a single regioisomer. Fortunately, the condensation afforded a single product **8**, and single X-ray crystallography³⁰ confirmed the correct regioisomer was obtained (insert). Subsequent Suzuki or Stille cross-

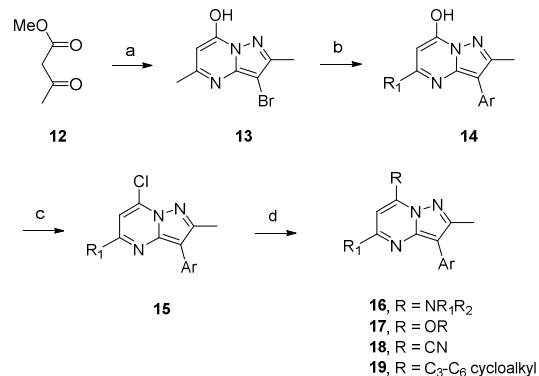
Scheme 1. Synthesis of Analogues **9**^a



^aReagents and conditions: (a) EtOH, mw, 110 °C, 30 min, 56-76%; (b) ArB(OR)₂, 10 mol% Pd(dppf)Cl₂, Cs₂CO₃, dioxane:water, mw, 150 °C, 30 min, 44-55% or ArSnBu₃, 5 mol% Pd(PPh₃)₄, PPh₃, CuBr, LiCl, dioxane, mw, 120 °C, 3h, 38-42%; (c) *bis*-pinacolborate, 5 mol% PdCl₂(PPh₃)₂, KOAc, dioxane, 100 °C, 16 h, 50-58% or *n*-BuLi, Bu₃SnCl, THF, 0 °C, 30 min, 84-93%.

coupling of **8**, with partners **11**, generated analogs **9** in moderate yields. To explore alternatives for the CF₃ moiety, additional chemistry was required (Scheme 2).³⁰ Here, a related condensation between **12** and **7** provided a single regioisomer **13**, which smoothly underwent cross-coupling reactions to deliver **14**. Treatment with POCl₃ gave the key chloro derivative **15** that could be diversified via either S_NAr reactions to introduce amines **16** and ethers **17** or palladium-catalyzed

Scheme 2. Synthesis of non-CF₃ Analogues **16**, **17**, **18** and **19**^a



^aReagents and conditions: (a) 4-bromo-3-methyl-1*H*-pyrazol-5-amine, AcOH, mw, 110 °C, 30 min, 68%; (b) ArB(OR)₂, 10 mol% Pd(dppf)Cl₂, Cs₂CO₃, dioxane:water, mw, 150 °C, 30 min, 26-38% (c) POCl₃, reflux, 30 min, 61-70%; (d) HNR₁R₂, EtOH, rt, 2h, 46-56%, or NaOR, ROH, rt, 30 min, 86-97%, or Zn(CN)₂, 5 mol% Pd(PPh₃)₄, NMP, 110 °C, 5h, 53-75%, or (cycloalkyl)ZnCl, 5 mol% Pd(PPh₃)₄, THF, reflux, 3h 74-83%.

organozinc chemistry to introduce either a nitrile **17** or cycloalkyl moieties **18** in good yields. All final compounds were >98% pure.

Evaluation of all of these analogs in our functional mGlu₇ assay highlighted extremely steep SAR, with the vast majority of the 100 analogues prepared devoid of mGlu₇ PAM activity

(Figure 3). Both the 7- CF_3 and 5- CH_3 moieties in **5** proved essential for mGlu₇ PAM activity, as all other substituents were inactive (mGlu₇ EC₅₀s >10 μM). The 2- CH_3 could be replaced with an ethyl moiety in **5**, but all other substituents lost mGlu₇ PAM activity. Thus, the only productive SAR resulted from functionalized aryl moieties in analogues **9**, where once again, the “fluorine walk” strategy² for allosteric modulator optimization proved fruitful (Table 1). Moreover, all analogs **9** evaluated for CNS penetration in the context of the broader SAR displayed favorable brain penetration ($K_{\text{p,s}} > 1$, $K_{\text{p,uu}} > 0.6$) in our high throughput rat plasma:brain level (PBL) cassette paradigm.²⁸

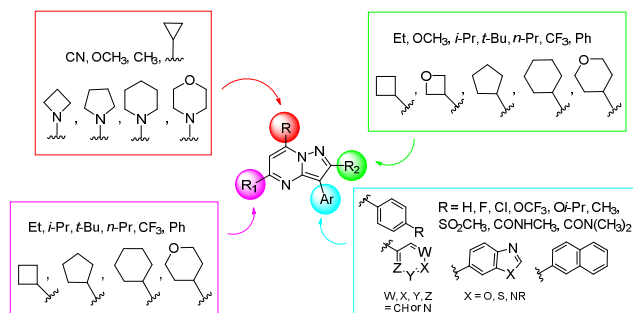
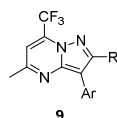


Figure 3. Substituents explored in analogs **9**, **16**, **17**, **18** and **19** that were inactive as mGlu₇ PAMs.

Table 1. Structures and Activities of Analogs **9**^a



Entry	Ar (Het)	R	mGlu ₇ EC ₅₀ (μM) ^a [% L-AP4 Max \pm SEM]	mGlu ₇ pEC ₅₀ (\pm SEM)	Rat K _p (K _{p,uu}) ^b
5		Me	3.3 [104 \pm 5]	5.48 \pm 0.14	1.4 (1.1)
9a		Me	>10 [20]	<5	ND
9b		Me	>10 [54]	<5	ND
9c		Me	1.5 [78 \pm 2]	5.82 \pm 0.06	4.3 (1.7)
9d		Me	1.7 [106 \pm 4]	5.78 \pm 0.10	1.4 (0.9)
9e		Me	0.60 [107 \pm 12]	6.22 \pm 0.11	2.2 (0.6)

9f		Me	0.65 [112 \pm 10]	6.19 \pm 0.14	4.3 (2.3)
9g		Me	1.0 [82 \pm 6]	5.99 \pm 0.06	2.7 (0.9)
9h		Me	0.48 [51 \pm 7]	6.32 \pm 0.06	ND
9i		Me	2.3 [87 \pm 6]	5.64 \pm 0.16	4.8 (1.7)
9j		Me	2.8 [91 \pm 3]	5.56 \pm 0.13	1.5 (0.8)
9k		Me	3.0 [98 \pm 7]	5.53 \pm 0.20	ND
9l		Et	1.7 [123 \pm 13]	5.76 \pm 0.16	ND
9m		Et	0.74 [102 \pm 4]	6.13 \pm 0.08	ND
9n		Et	1.05 [113 \pm 5]	5.98 \pm 0.08	ND
9o		Et	1.48 [102 \pm 6]	5.83 \pm 0.10	ND

^aCalcium mobilization assays with rat mGlu₇/G_{q15}-HEK cells performed in the presence of an EC₂₀ fixed concentration of L-AP4; values represent means from three ($n=3$) independent experiments performed in triplicate. ^bTotal and calculated unbound brain:plasma partition coefficients determined at 0.25 h post-administration of an IV cassette dose (0.20–0.25 mg/kg) to male, SD rats ($n=1$), in conjunction with *in vitro* rat plasma protein and brain homogenate binding assay data. ND = not determined.

As discussed previously, HTS hit **5** exhibited improved selectivity for mGlu₇ over previous compounds VU0155094 and VU0422288 (mGlu₇ EC₅₀ for **5** = 3.3 μM , pEC₅₀ = 5.48 \pm 0.14, 104 \pm 5 L-AP4 Max, mGlu₄ EC₅₀ >10 μM , mGlu₈ EC₅₀ >10 μM) and displayed exceptional CNS penetration (rat plasma:brain K_p = 1.4, K_{p,uu} = 1.1). Moving the methoxy group to either the 2- or 3-position, as in **9a** and **9b**, respectively, led to inactive analogs, as did a wide-range of substituents across multiple domains of **5** (Figure 3). When steep SAR has presented in other GPCR allosteric modulator programs, application of the ‘fluorine walk’ strategy³¹ has proven beneficial, and this is true for the present series. The addition

of a single fluorine atom to either the 2- or 3-position of the 4-methoxy phenyl moiety increased mGlu₇ PAM activity (**9c**, mGlu₇ EC₅₀ = 1.5 μM, and **9d**, mGlu₇ EC₅₀ = 1.7 μM), respectively. In the case of **9c**, K_p (4.3) and K_{p,uu} (1.7) improved as well relative to **5**. The addition of two fluorine atoms to the 4-methoxy phenyl moiety afforded even more favorable results. Here, the 2,6-difluoro congener **9e** (mGlu₇ EC₅₀ = 0.60 μM, pEC₅₀ = 6.22±0.11, 107±12 L-AP4 Max) and the 2,3-difluoro derivative **9f** (mGlu₇ EC₅₀ = 0.65 μM, pEC₅₀ = 6.19±0.14, 112±10 L-AP4 Max) provided submicromolar mGlu₇ PAM EC₅₀s and good CNS penetration (K_ps of 2.2 (K_{p,uu} = 0.6) and 4.3 (K_{p,uu} = 2.3) for **9e** and **9f**, respectively). The 2-chloro-5-fluoro analog **9h** was the most potent mGlu₇ PAM in the series (mGlu₇ EC₅₀ = 0.48 μM, pEC₅₀ = 6.32±0.06, but the efficacy was diminished (51±7 L-AP4 Max). Difluoromethyl ether congeners **9j** and **9k** were also active, but solubility concerns precluded further advancement.

The *in vitro* DMPK profiles (Table 2) and K_p/K_{p,uu}s of **5** and analogs **9** were tightly conserved in terms of predicted hepatic clearance, protein binding, and CYP450 inhibition (note, the chemotype engenders 1A2 inhibition); thus, physicochemical properties of individual PAMs and mGlu₇ PAM potency/efficacy assisted in prioritization. Attention then focused on further characterization of **9e** and **9f** as potential mGlu₇ PAM *in vivo* tool compounds. Both PAMs **9e** and **9f** were predicted to be moderate to highly cleared in rat (CL_{hep} = 64.2 and 65.5 mL/min/kg, respectively), and both displayed good free fraction in rat plasma (f_u = 0.05 and 0.02; rat brain f_us of 0.014 and 0.012) and clean CYP450 profiles (**9e**: >30 μM versus 3A4, 2D6 and 2C9, 8.7 μM at 1A2; **9f**: >30 μM versus 3A4, 2D6, 24.6 μM at 2C9 and 3.1 μM at 1A2). Based on the improved rat K_p/K_{p,uu}, **9f** was further advanced into a mouse PBL time-course study. Here, a 10 mg/kg IP dose of **9f** was followed out to 6 hours with non-serial sampling of both plasma and brain at each selected time point, and displayed excellent CNS penetration (K_p @ 60 min of 2.1 and K_p @ 360 min of 1.1). Thus, for a first generation *in vivo* tool compound, **9f** could be studied in both rat and mouse models.

Table 2. *In vitro* DMPK Profiles of **5** and Analogs **9**

Property	5	9c	9e	9f	9g
MW	321	339	357	357	357
cLogP	3.70	3.78	4.11	3.90	3.97
TPSA	43.2	37.2	37.2	37.2	37.2
<i>In vitro</i> PK parameters					
CL _{HEP} (mL/min/kg), rat	59.4	62.1	64.2	65.5	63.0
CL _{HEP} (mL/min/kg), human	18.8	18.5	14.2	16.6	15.0
Rat f _{u,plasma}	0.021	0.030	0.046	0.022	0.046
Human f _{u,plasma}	0.006	0.013	0.016	0.008	0.002
Rat f _{u,brain}	0.016	0.012	0.014	0.012	0.015
Cytochrome P ₄₅₀ (IC ₅₀ , μM)					
1A2	0.69	0.33	8.67	3.08	2.93
2C9	>30	27	>30	24.7	>30
2D6	>30	>30	>30	>30	>30

3A4	>30	>30	>30	>30	>30
-----	-----	-----	-----	-----	-----

However, broader mGlu receptor selectivity, as well as general ancillary pharmacology, needed to be assessed prior to any *in vivo* work. Gratifyingly, **9f** was inactive (EC₅₀/IC₅₀s > 10 μM) against mGlu_{1,2,3,4,5} and 6, but mGlu₈ activity was present (mGlu₈ EC₅₀ = 2.6 μM, pEC₅₀ = 5.58±0.06, 101±2 Glu Max, Table 3). Interestingly, **9f** was inactive at the other Group III mGlus (mGlu₄ and mGlu₆, see supporting data).³⁰ These data prompted us to examine mGlu selectivity for other analogues in this series, and, in general, as PAM potency at mGlu₇ increased, mGlu₈ PAM activity also increased (Table 3); however, PAM activity at mGlu_{4/6} remained weak to inactive (data not shown).³⁰ PAM **9f** represents a missing link in the Group III receptor PAM toolbox and serves as a nice complement to the mGlu_{4/8} PAM, **1**. In addition, broader ancillary pharmacology was assessed in a Eurofins Lead profiling panel³⁰ of 68 GPCRs, ion channels and transporters, and a single activity assessment at NK1 (K_i = 650 nM, functional antagonist IC₅₀ of 3.4 μM) proved significant (all others <50% inhibition of radioligand binding at 10 μM).³¹

Table 3. Comparison of potency and % maximal agonist response across the three widely expressed CNS group III mGlu receptors for **5**, **9f** and related analogs.

Entry	mGlu ₄ EC ₅₀ (μM) [% agonist Max ±SEM]	mGlu ₄ pEC ₅₀ (±SEM)	mGlu ₇ EC ₅₀ (μM) [% agonist Max ±SEM]	mGlu ₇ pEC ₅₀ (±SEM)	mGlu ₈ EC ₅₀ (μM) [% agonist Max ±SEM]	mGlu ₈ pEC ₅₀ (±SEM)
5	>10 [48±3]	<5	3.3 [104±5]	5.48±0.14	>10 [86±5]	<5
9c	>30	<4.5	1.5 [78±2]	5.82±0.06	2.0 [70±6]	5.69±0.13
9e	>10 [69±3]	<5	0.60 [107±12]	6.22±0.11	2.9 [101±1]	5.54±0.18
9f	>10 [45±3]	<5	0.65 [112±10]	6.19±0.14	2.6 [101±2]	5.58±0.06
9h	>30	<4.5	0.48 [51±7]	6.32±0.06	0.49 [41±10]	6.31±0.06
9m	2.1 [53±6]	5.67±0.07	0.74 [102±4]	6.13±0.08	0.89 [85±6]	6.05±0.09

With the first mGlu₇-preferring, and highly CNS penetrant, PAM in hand, we assessed the activity of **9f** in a standard rat preclinical model predictive of antipsychotic activity, amphetamine-induced hyperlocomotion (AHL),³² as human genetic association studies have identified *GRM7* polymorphisms linked to schizophrenia.^{13,19} In this study, **9f** was dosed at 30 mg/kg IP in 10% Tween 80/H₂O (0.75 mg/kg. s.c. amphetamine), and there was no efficacy observed in this assay (data not shown).³⁰ Terminal (t = 2 hr) plasma and brain samples were taken, and **9f** displayed a terminal K_p of 2.43 with total brain levels ~9x above the mGlu₇ PAM *in vitro* EC₅₀. These data represent the first evaluation of an mGlu_{7/8} PAM in rat AHL, but the lack of efficacy here does not rule out potential efficacy with NMDA antagonist challenge³³ or in other antipsychotic models (prepulse inhibition, conditioned avoidance responding, etc. or other genetic models (all of which are under pursuit)). As cognition deficits are another major, and

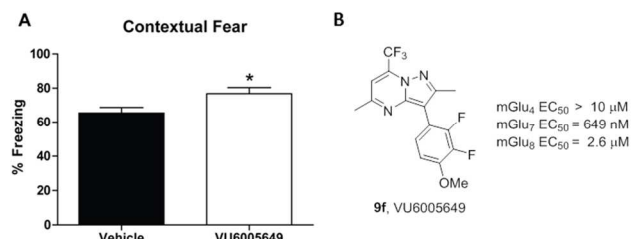


Figure 4. **9f**, VU6005649, administration has pro-cognitive effects on associative learning in wild type mice. **A)** Contextual Fear Conditioning. Vehicle (10% Tween 80, $n = 11$) or **9f** (VU6005649, 50 mg/kg, $n = 11$) was administered (i.p.) to mice 15 minutes prior to training. On test day, VU6005649-treated mice froze significantly more than vehicle-treated mice (vehicle: $65.5 \pm 3.3\%$ vs. VU6005649: $76.8 \pm 3.6\%$, $p = 0.03$) indicative of procognitive compound effects on associative learning. Two tailed Students t-test. Values presented as mean \pm SEM.

unmet, symptom cluster in schizophrenia, we next evaluated **9f** in a standard mouse contextual fear conditioning (CFC) model at 50 mg/kg IP.³⁰ Here, **9f** showed modest but significant pro-cognitive effects on associative learning in wild type mice (**Figure 4**), and the first example of efficacy of an mGlu_{7/8} PAM in this model. We would note that the compound did induce some level of sedation, which was still present when the compound was evaluated in mGlu₇ knockout mice (data not shown). As sedation during training would be predicted to diminish the capacity for associative learning, it is likely that the full efficacy of PAM **9f** in this cognitive assay was masked by off-target effects (such as NK1). Such results suggest that the utility of this tool may be limited in certain *in vivo* assays. Moreover, these exciting data warrant further optimization of this and other HTS hits to develop a highly selective mGlu₇ PAM for further *in vivo* target validation studies.

PAM **9f**, an mGlu_{7/8} PAM, and the first reported mGlu₇ preferring PAM, complements existing Group III mGlu receptor PAM tool compounds **1-4**, and represents a major advance in the field. This novel series of pyrazolo[1,5-*a*]pyrimidines possess good free fraction and CNS penetration, lending utility as both *in vitro* and *in vivo* tool compounds alone or in combination studies with **1-4** and *Grm7*^{-/-} mice. Additional behavioral pharmacology with **9f**, and optimization of additional hits from the HTS screen, are underway and will be reported in due course.

AUTHOR INFORMATION

Corresponding Authors

* (CMN). Phone: 1 615-343-4303. Fax: 1 615-936-4381. Email: colleen.niswender@vanderbilt.edu.

* (CWL). Phone: 1 615-322-8700. Fax: 1 615-936-4381. Email: craig.lindsley@vanderbilt.edu.

Author Contributions

CWL, CMN, PJC, and RGG drafted/corrected the manuscript. MA, MS, KAB and DWE performed the chemical synthesis. CWL, PJC, CMN, CJK, and ALR oversaw the target selection and interpreted the biological data. ML and ALR performed the *in vitro* molecular pharmacology studies. ALB and SC performed the *in vitro* and *in vivo* DMPK studies. CKJ, MB and RGG performed the *in vivo* experiments. All authors have approved the manuscript.

Acknowledgement

The authors would like to thank the NIH/NIMH MH102548 (to C.M.N.) and MH113543 (to C.M.N. and C.W.L.) and the William K. Warren, Jr. and the William K. Warren Foundation who funded the William K. Warren, Jr. Chair in Medicine (to C.W.L.). We would like to thank the Vanderbilt High Throughput Screening Facility for their assistance with primary screening.

ASSOCIATED CONTENT

Supporting Information. General methods for the synthesis and characterization of all compounds, and methods for the *in vitro* and *in vivo* DMPK protocols and supplemental figures and detailed explanation of the sedation studies. This material is available free of charge via the Internet at <http://pubs.acs.org>.

ABBREVIATIONS

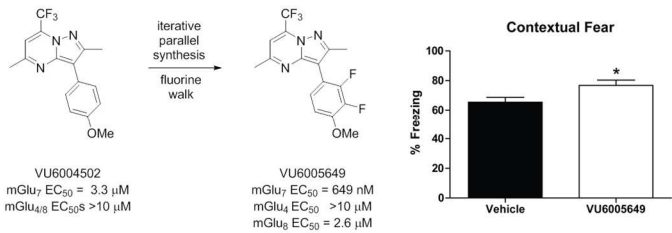
AHL, amphetamine-induced hyperlocomotion; metabotropic glutamate receptor (mGlu); PAM, positive allosteric modulator; NAM, negative allosteric modulator; HTS, high-throughput screen; CFC, contextual fear conditioning; PBL, plasma:brain level; RTT, Rett Syndrome; CNS, central nervous system; mGlu7, metabotropic glutamate receptor subtype 7; ADHD, attention deficit hyperactivity disorder

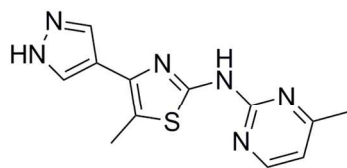
REFERENCES

- Niswender, C.M. and Conn, P.J. Metabotropic glutamate receptors: physiology, pharmacology, and disease. *Annu. Rev. Pharmacol. Toxicol.* **2010**, *50*, 295–322.
- Lindsley, C.W.; Emmitte, K.A.; Hopkins, C.R.; Bridges, T.M.; Gregory, K.A.; Niswender, C.M.; Conn, P.J. Practical strategies and concepts in GPCR allosteric modulator discovery: Recent advances with metabotropic glutamate receptors. *Chem. Rev.* **2016**, *116*, 6707–6741.
- Sansig, G.; Bushell, T. J.; Clarke, V. R.; Rozov, A.; Burnashev, N.; Portet, C.; Gasparini, F.; Schmutz, M.; Klebs, K.; Shigemoto, R.; Flor, P. J.; Kuhn, R.; Knoepfel, T.; Schroeder, M.; Hampson, D. R.; Collett, V. J.; Zhang, C.; Duvoisin, R. M.; Collingridge, G. L.; van Der Putten, H. Increased seizure susceptibility in mice lacking metabotropic glutamate receptor 7. *J. Neurosci.* **2001**, *21*, 8734–8745.
- Goddyn, H.; Callaerts-Vegh, Z.; Stroobants, S.; Dirikx, T.; Vansteenkoven, D.; Hermans, D.; van der Putten, H.; D'Hooge, R. Deficits in acquisition and extinction of conditioned responses in mGluR7 knockout mice. *Neurobiol. Learn. Mem.* **2008**, *90*, 103–111.
- Palucha, A.; Klak, K.; Branski, P.; van der Putten, H.; Flor, P.J.; Pilc, A. Activation of the mGlu7 receptor elicits antidepressant-like effects in mice. *Psychopharmacology* **2007**, *194*, 555–562.
- Callaerts-Vegh, Z.; Beckers, T.; Ball, S.M.; Baeyens, F.; Callaerts, P.F.; Cryan, J.F.; Molnar, E.; D'Hooge, R. Concomitant deficits in working memory and fear extinction are functionally dissociated from reduced anxiety in metabotropic glutamate receptor 7-deficient mice. *J. Neurosci.* **2006**, *26*, 6573–6582.
- Mitsukawa, K.; Mombereau, C.; Lotscher, E.; Uzunov, D.P.; van der Putten, H.; Flor, P.J.; Cryan, J.F. Metabotropic Glutamate Receptor Subtype 7 Ablation Causes Dysregulation of the HPA Axis and In-

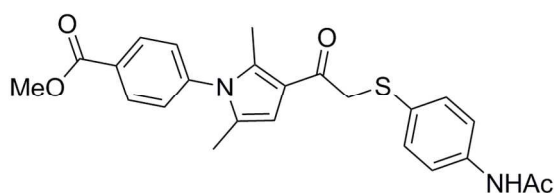
- creases Hippocampal BDNF Protein Levels: Implications for Stress-Related Psychiatric Disorders. *Neuropsychopharmacology* **2006**, *31*, 1112-1122.
8. Holscher, C.; Schmid, S.; Pilz, P.K.; Sansig, G.; van der Putten, H.; Plappert, C.F. Lack of the metabotropic glutamate receptor subtype 7 selectively modulates Theta rhythm and working memory. *Learn Mem* **2005**, *12*, 450-455.
 9. Holscher, C.; Schmid, S.; Pilz, P.K.; Sansig, G.; van der Putten, H.; Plappert, C.F. Lack of the metabotropic glutamate receptor subtype 7 selectively impairs short-term working memory but not long-term memory. *Behav. Brain Res.* **2004**, *154*, 473-481.
 10. Bushell, T.J.; Sansig, G.; Collett, V.J.; van der Putten, H.; Collingridge, G.L. Altered short-term synaptic plasticity in mice lacking the metabotropic glutamate receptor mGlu7. *ScientificWorldJournal* **2002**, *2*, 730-737.
 11. Masugi, M.; Yokoi, M.; Shigemoto, R.; Muguruma, K.; Watanabe, Y.; Sansig, G.; van der Putten, H.; Nakanishi, S. Metabotropic glutamate receptor subtype 7 ablation causes deficit in fear response and conditioned taste aversion. *J. Neurosci.* **1999**, *19*, 955-963.
 12. Breen, G.; Webb, B.T.; Butler, A.W.; van den Oord, E.J.; Tozzi, F.; Craddock, N.; Gill, M.; Korszun, A.; Maier, W.; Middleton, L.; Mors, O.; Owen, M. J.; Cohen-Woods, S.; Perry, J.; Galwey, N. W.; Upmanyu, R.; Craig, I.; Lewis, C. M.; Ng, M.; Brewster, S.; Preisig, M.; Rietschel, M.; Jones, L.; Knight, J.; Rice, J.; Muglia, P.; Farmer, A. E.; McGuffin, P. A genome-wide significant linkage for severe depression on chromosome 3: the depression network study. *Am. J. Psychiatry* **2011**, *168*, 840-847.
 13. Ganda, C.; Schwab, S. G.; Amir, N.; Heriani, H.; Irmansyah, I.; Kusumawardhani, A.; Nasrun, M.; Widyawati, I.; Maier, W.; Wildenauer, D. B. A family-based association study of DNA sequence variants in GRM7 with schizophrenia in an Indonesian population. *Int. J. Neuropsychopharmacol.* **2009**, *12*, 1283-1289.
 14. Mick, E.; Neale, B.; Middleton, F. A.; McGough, J. J.; Faraone, S. V. Genome-wide association study of response to methylphenidate in 187 children with attention-deficit/hyperactivity disorder. *Am. J. Med. Genet., Part B* **2008**, *147B*, 1412-1418.
 15. Yang, Y. and Pan, C. Role of metabotropic glutamate receptor 7 in autism spectrum disorders: a pilot study. *Life Sci.* **2013**, *92*, 149-153.
 16. Elia, J.; Glessner, J.T., et al. Genome-wide copy number variation study associated metabotropic glutamate receptor gene networks with attention deficit hyperactivity disorder. *Nat. Genetics* **2012**, *44*, 78-84.
 17. Douglas, L.N.; McGuire, A.B.; Manzardo, A.M.; Butler, M.G. High-resolution chromosome ideogram representation of recognized genes for bipolar disorder. *Gene* **2016**, *586*, 136-147.
 18. Shyn, S.I.; Shi, J.; Kraft, J.B.; Potash, J.B.; Knowles, J.A.; Weissman, M.M.; Garriock, H.A.; Yokoyama, J.S.; McGrath, P.J.; Peters, E.J.; Scheftner, W.A.; Coryell, W.; Lawson, W.B.; Jancic, D.; Gejman, P.V.; Sanders, A.R.; Holmans, P.; Slager, S.L.; Levinson, D.F.; Hamilton, S.P. Novel loci for major depression identified by genome-wide association study of Sequenced Treatment Alternatives to Relieve Depression and meta-analysis of three studies. *Mol. Psychiatry* **2011**, *16*, 202-215.
 19. Li, W.; Ju, K.; Li, Z.; He, K.; Chen, J.; Wang, Q.; Yang, B.; An, L.; Feng, G.; Sun, W.; Zhou, J.; Zhang, S.; Song, P.; Khan, R.; Ji, W.; Shi, Y. Significant association of GRM7 and GRM8 genes with schizophrenia and major depressive disorder in the Han Chinese population. *Eur. Neuropsychopharmacol.* **2016**, *26*, 136-146.
 20. Park, S.; Kim, B.N.; Cho, S.C.; Kim, J.W.; Kim, J.I.; Shin, M.S.; Yoo, H.J.; Han, D.H.; Cheong, J.H. The metabotropic glutamate receptor subtype 7 rs3792452 polymorphism is associated with the response to methylphenidate in children with attention-deficit/hyperactivity disorder. *J. Child Adolesc. Psychopharmacol.* **2014**, *24*, 223-227.
 21. Park, S.; Jung, S.W.; Kim, B.N.; Cho, S.C.; Shin, M.S.; Kim, J.W.; Yoo, H.J.; Cho, D.Y.; Chung, U.S.; Son, J.W.; Kim, H.W. Association between GRM7 rs3792452 polymorphism and attention-deficit/hyperactivity disorder in a Korean sample. *Behav. Brain Funct.* **2013**, *9*, 1-11.
 22. Kandaswamy, R.; McQuillin, A.; Curtis, D.; Gurling, H. Allelic association, DNA resequencing and copy number variation at the metabotropic glutamate receptor GRM7 gene locus in bipolar disorder. *Am. J. Genet. B Neuropsychiatr. Genet.* **2014**, *165B*, 365-372.
 23. Liu, Y.; Zhang, Y.; Zhao, D.; Dong, R.; Yang, X.; Tammimies, K.; Uddin, M.; Scherer, S.W.; Gai, Z. Rare de novo deletion of metabotropic glutamate receptor 7 (GRM7) gene in a patient with autism spectrum disorder. *Am. J. Genet. B Neuropsychiatr. Genet.* **2015**, *168B*, 258-264.
 24. Charnig, W.L.; Karaca, E.; Coban-Akdemir, Z.; Gambin, T.; Atik, M.M.; Gu, S.; Posey, J.E.; Jhangiani, J.A.; Muzny, D.M.; Doddapaneni, H.; Hu, J.; Boerwinkle, E.; Gibbs, R.A.; Rosenfeld, J.A.; Cui, H.; Xia, F.; Manickam, K.; Yang, Y.; Faqeih, E.A.; Al Asmari, A.; Saleh, M.A.; El-Hattab, A.W.; Lupski, J.R. Exome sequencing in mostly consanguineous Arab families with neurological disease provides a high potential molecular diagnosis rate. *BMC Med. Genomics* **2016**, *19*, 42-54.
 25. Reuter, M.S.; Tawamie, H., et al. Diagnostic yield and novel candidate genes by exome sequencing in 152 consanguineous families with neurodevelopmental disorders. *JAMA Psychiatry* **2017**, *74*, 293-299.
 26. Gogliotti R.G., Senter R.K., Fisher N.M., Adams J., Zamorano R., Walker A.G., Blobaum A.L., Engers D.W., Hopkins C.R., Daniels J.S., Jones, C.K., Lindsley C.W., Xiang Z., Conn P.J., and Niswender C.M. Metabotropic Glutamate Receptor 7 Allosteric Modulation Rescues Long Term Potentiation, Cognition and Apneas in Mecp2-Deficient Mice. *Sci. Trans. Med.* **2017**, *9*, eaai7549.
 27. Jalan-Sakrikar, N.; Field, J.R.; Klar, R.; Mattmann, M.E.; Gregory, K.J.; Zamorano, R.; Engers, D.W.; Bollinger, S.R.; Weaver, C.D.; Days, E.; Lewis, L.M.; Utley, T.J.; Hurtado, M.; Rigault, D.; Acher, F.; Walker, A.G.; Melancon, B.J.; Wood, M.R.; Lindsley, C.W.; Conn, P.J.; Xiang, Z.; Hopkins, C.R.; Niswender, C.M. Identification of positive allosteric modulators VU0155094 (ML397) and VU0422288 (ML396) reveals new insights into the biology of metabotropic glutamate receptor 7. *ACS Chem. Neurosci.* **2014**, *5*, 1221-1237.
 28. Le Poul, E.; Bolea, C.; Girarg, F.; Poli, S.; Charvin, D.; Campo, B.; Bortoli, J.; Bessif, A.; Luo, B.; Koser, A.J.; Hodge, L.M.; Smith, K.M.; DiLella, A.G.; Liverton, N.; Hess, F.; Browne, S.E.; Reynolds, I.J. A potent and selective metabotropic glutamate receptor 4 positive allosteric modulator improves movement in rodent models of Parkinson's disease. *J. Pharmacol. Exp. Ther.* **2012**, *343*, 167-177.
 29. Kalinichev, M.; Rouillier, M.; Girard, F.; Royer-Urios, I.; Bournique, B.; Finn, T.; Charvin, D.; Campo, B.; Le Poul, E.; Mutel, V.; Poli, S.; Neale, S.A.; Salt, T.E.; Lutjens, R. ADX71743, a potent and selective negative allosteric modulator of metabotropic glutamate receptor 7: in vitro and in vivo characterization. *J. Pharmacol. Exp. Ther.* **2013**, *3*, 624-636.
 30. See Supporting Information for full experimental details.
 31. For details see: www.eurofin.com
 32. Bubser, M.; Bridges, T.M.; Denker, D.; Gould, R.W.; Grannan, M.; Noetzel, M.J.; Lamsal, A.; Niswender, C.M.; Daniels, J.S.; Poslusney, M.S.; Melancon, B.J.; Tarr, J.C.; Byers, F.W.; Wess, J.; Duggan, M.E.; Dunlop, J.; Wood, M.W.; Brandon, N.J.; Wood, M.R.; Lindsley, C.W.; Conn, P.J.; Jones C.K. Selective activation of M₄ muscarinic acetylcholine receptors reverses MK-801-induced behavioral impairments and enhances associative learning in rodents. *ACS Chem. Neurosci.* **2014**, *5*, 920-942.

Table of Contents Graphic

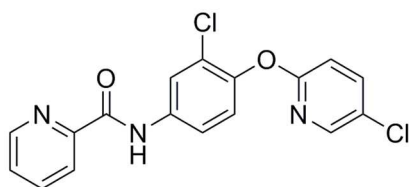




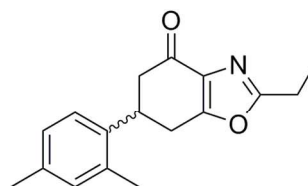
1, ADX88178
mGlu₄ EC₅₀ = 52 nM
mGlu₇ EC₅₀ >10 μM
mGlu₈ EC₅₀ = 1.2 μM



2, VU0155094
mGlu₄ EC₅₀ = 3.2 μM
mGlu₇ EC₅₀ = 1.5 μM
mGlu₈ EC₅₀ = 900 nM

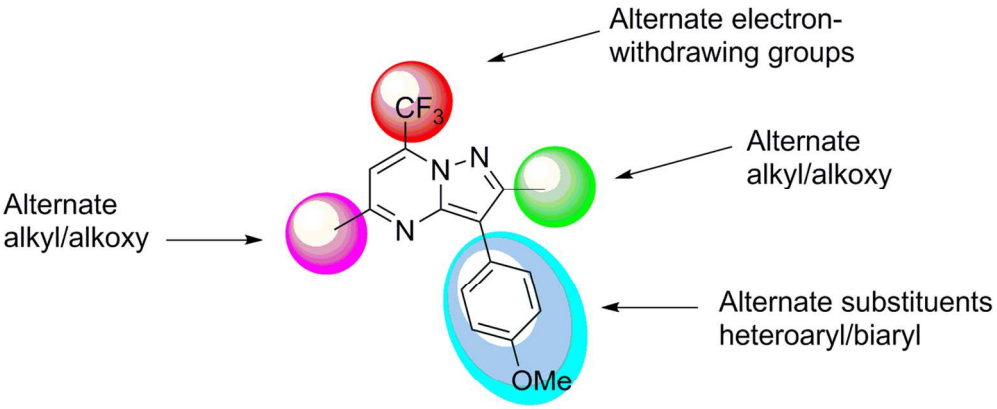


3, VU0422288
mGlu₄ EC₅₀ = 108 nM
mGlu₇ EC₅₀ = 146 nM
mGlu₈ EC₅₀ = 125 nM



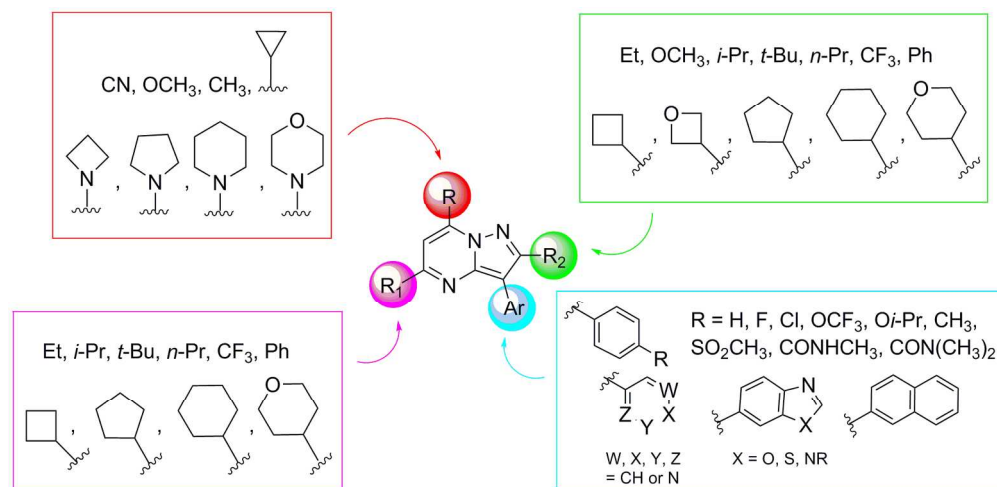
4, ADX71743
mGlu₄ IC₅₀ >10 μM
mGlu₇ IC₅₀ = 650 nM
mGlu₈ IC₅₀ >10 μM

137x112mm (300 x 300 DPI)

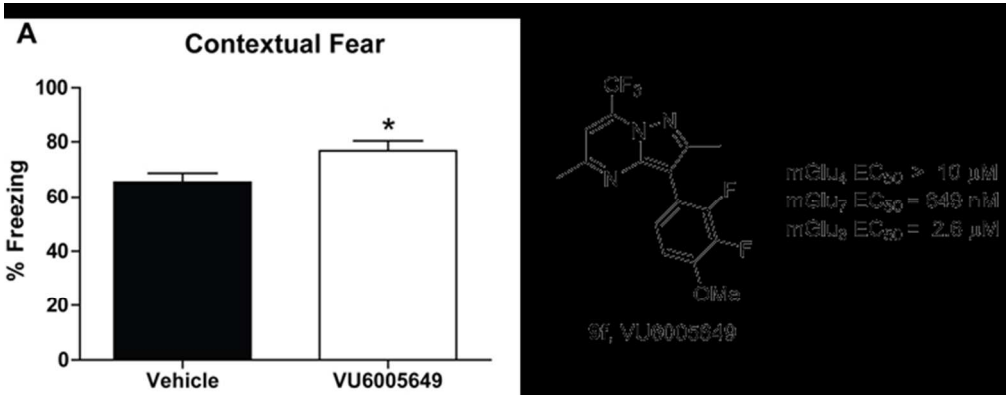


5, VU6004502
mGlu₇ EC₅₀ = 3.3 μM
mGlu_{4/8} EC₅₀s >10 μM

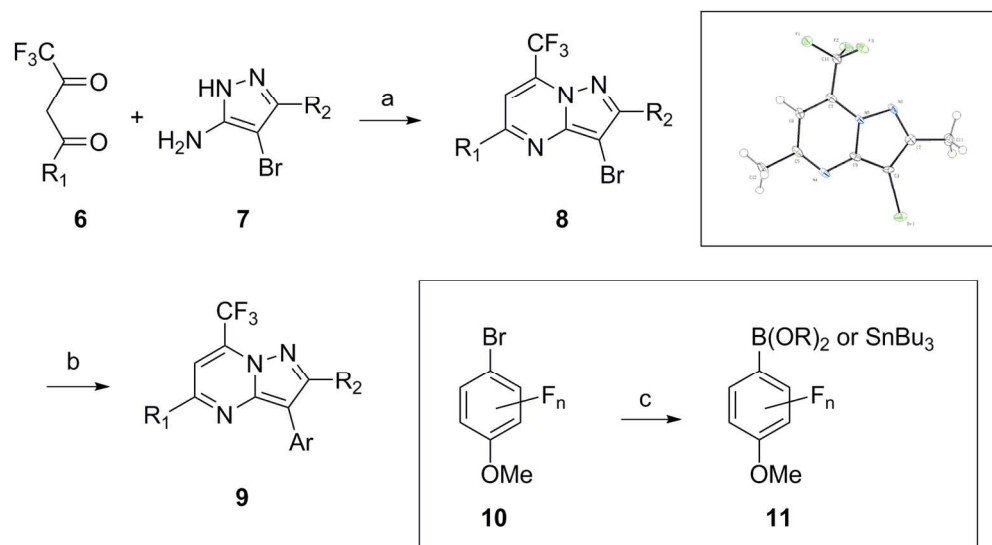
124x71mm (300 x 300 DPI)



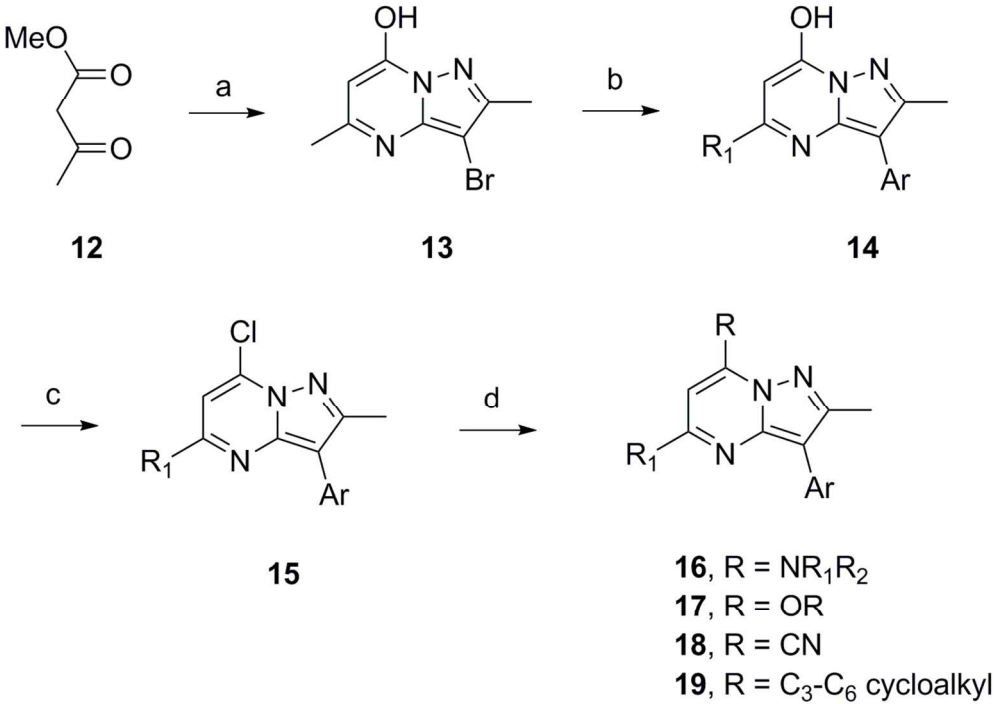
171x84mm (300 x 300 DPI)



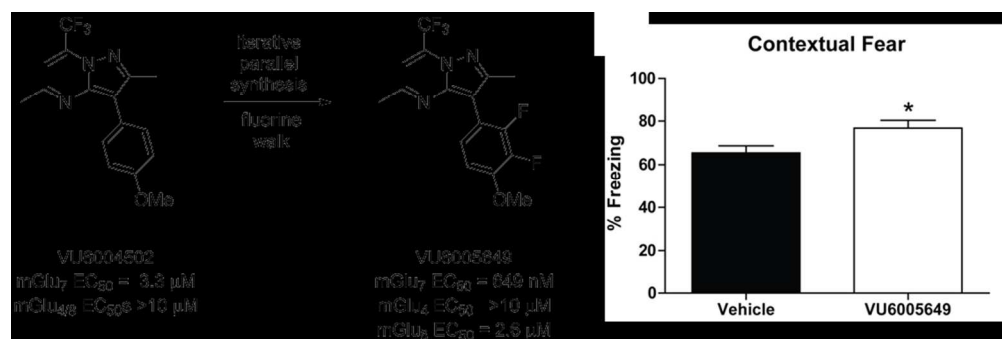
127x50mm (150 x 150 DPI)



145x80mm (300 x 300 DPI)



118x84mm (300 x 300 DPI)



192x64mm (150 x 150 DPI)